Molecular Pharmacology Fast Forward. Published on October 14, 2014 as DOI: 10.1124/mol.114.094722
This article has not been copyedited and formatted. The final version may differ from this version.

Influence of $G\alpha_q$ on the dynamics of M_3-ACh-receptor-GRK2 interaction

Valerie Wolters, Cornelius Krasel, Jörg Brockmann, Moritz Bünemann

Institute for Pharmacology and Clinical Pharmacy, Faculty of Pharmacy, Philipps-University Marburg, Karl-von-Frisch-Str. 1, 35043 Marburg, Germany (V.W., C.K., M.B.)

Department of Pharmacology and Toxicology, University of Würzburg, Versbacher Str. 9, 97078 Würzburg, Germany (J.B.)

Molecular Pharmacology Fast Forward. Published on October 14, 2014 as DOI: 10.1124/mol.114.094722
This article has not been copyedited and formatted. The final version may differ from this version.

Running title: $G\alpha_q$-effects on M_3-ACh-receptor-GRK2 interaction

Corresponding author:

Moritz Bünemann, Institute for Pharmacology and Clinical Pharmacy, Faculty of Pharmacy, Philipps-University Marburg, Karl-von-Frisch-Str. 1, 35043 Marburg, Germany,

Tel. +49 6421 2825773, Fax +49 6421 2825720, moritz.buenemann@staff.uni-marburg.de

Number of text pages: 28

Number of tables: 0

Number of figures: 6 + 4 supplemental figures

Number of references: 31

Number of words in the Abstract: 237

Number of words in the Introduction: 526

Number of words in the Discussion: 871

Abbreviations: α_{2A}-AR, α_{2A}-adrenergic receptor; ACh, acetylcholine; AChR, acetylcholine receptor; CFP, cyan fluorescent protein; FRET, Förster resonance energy transfer; GRK, G-protein-coupled receptor kinase; HEK, human embryonic kidney; mTurq, mTurquoise fluorescent protein; YFP, yellow fluorescent protein

Molecular Pharmacology Fast Forward. Published on October 14, 2014 as DOI: 10.1124/mol.114.094722
This article has not been copyedited and formatted. The final version may differ from this version.

Abstract

G-protein-coupled receptor kinase 2 (GRK2) is a serine/threonine kinase with an important function in the desensitisation of G-protein-coupled receptors. Based on its ability to bind G-protein βγ subunits as well as activated $G\alpha_q$ subunits it can be considered as an effector for G-proteins. The recruitment of GRK2 to activated receptors is well-known to be mediated by Gβγ together with negatively charged membrane phospholipids. In the current study we address the role of $G\alpha_q$ on the interaction of GRK2 with activated G_q-protein-coupled receptors. Therefore, we established new FRET-based assays to study the interaction of GRK2 with the M_3-ACh receptor as well as G_q-protein subunits with high spatio-temporal resolution in single living HEK293T cells. M_3-ACh receptor stimulation with 10 µM acetylcholine resulted in distinct changes in FRET, which reflects interaction of the respective proteins. GRK2 mutants with reduced binding-affinity towards $G\alpha_q$ (GRK2(D110A)) and Gβγ (GRK2(R587Q)) were utilised in order to determine the specific role of G_q-protein-binding by GRK2. Comparison of absolute FRET amplitudes demonstrated that $G\alpha_q$ enhances the extent and stability of the GRK2-M_3-ACh receptor interaction and that not only Gβγ but also $G\alpha_q$ can target GRK2 to the membrane. This reveals an important role of $G\alpha_q$ in efficient recruitment of GRK2 to M_3-ACh receptors. Furthermore, interactions between $G\alpha_q$ and GRK2 were associated with a prolongation of the interaction between GRK2 and the M_3-ACh receptor and enhanced arrestin recruitment by these receptors, indicating that $G\alpha_q$ influences signalling and desensitisation.

Molecular Pharmacology Fast Forward. Published on October 14, 2014 as DOI: 10.1124/mol.114.094722
This article has not been copyedited and formatted. The final version may differ from this version.

Introduction

G-protein-coupled receptor kinases (GRKs) are a family of serine/threonine kinases that initiate the desensitisation of G-protein-coupled receptors. By phosphorylating cytoplasmic regions of the receptor they induce binding of arrestin proteins to activated receptors, resulting in an uncoupling of receptor signalling and initiation of receptor internalisation (Wu et al., 1998; Krupnick and Benovic, 1998). Most GRKs are ubiquitously expressed (Pitcher et al., 1998) and alterations in their expression levels have been shown to be associated with several diseases such as heart failure (Hata and Koch, 2003; Ungerer et al., 1993). The important influence of GRKs in the cardiovascular system and other fields demonstrates that a comprehensive knowledge about the various functions of GRKs is of great interest.

Structurally, GRKs are multi-domain proteins, containing an N-terminal RGS homology domain, followed by a central kinase domain and a C-terminal domain (Pitcher et al., 1998). The C-terminal domain is variable between the different GRKs, but in all cases essential for their membrane targeting. GRK2 and GRK3 contain the largest C-terminal domain including a pleckstrin homology domain that interacts with $G\beta\gamma$ subunits as well as negatively charged membrane phospholipids (Pitcher et al., 1992; Touhara et al., 1995). Because of overlapping binding sites, these GRKs compete with inactive $G\alpha_q$ subunits for $G\beta\gamma$ binding. Therefore, they only interact with $G\beta\gamma$ and translocate to the membrane after G-protein activation (Ford et al., 1998).

The RGS homology domain of GRK2 and GRK3 is known to interact with activated $G\alpha_q$-proteins, but not with $G\alpha_s$- or $G\alpha_i$-proteins (Carman et al., 1999; Sallese et al., 2000). It has been shown by a crystal structure that even a simultaneous binding of $G\beta\gamma$ and $G\alpha_q$ is possible (Tesmer et al., 2005). The GRK binding site on $G\alpha_q$ includes the $G\alpha_q$ switching-region, which enables the discrimination between the active and inactive state of $G\alpha_q$ (Carman et al., 1999). The GRK surface that binds $G\alpha_q$ (C-site) differs from the binding site RGS proteins use (A-

Molecular Pharmacology Fast Forward. Published on October 14, 2014 as DOI: 10.1124/mol.114.094722
This article has not been copyedited and formatted. The final version may differ from this version.

site (Zhong and Neubig, 2001)) (Sterne-Marr et al., 2003), which is a possible explanation for the weak to no GAP function of GRK2 (Carman et al., 1999). The sequestration of activated G-protein subunits by GRK2 has been shown to desensitise the signalling of G-protein coupled receptors phosphorylation-independently by preventing their interaction with downstream effectors (Fernandez et al., 2011; Raveh et al., 2010). However, whether binding of activated $G\alpha_q$ affects the function of GRK2 is still unknown and needs further investigation.

With the present study we aimed to clarify the effects of $G\alpha_q$ on the interaction of GRK2 with activated G_q-protein-coupled receptors. Of special importance for our study were previously published GRK2 mutants with reduced binding-affinity towards $G\alpha_q$ (GRK2(D110A) (Sterne-Marr et al., 2003)) and $G\beta\gamma$ (GRK2(R587Q) (Carman et al., 2000)). These mutants allowed determination of the individual contribution of the G_q-protein subunits for the recruitment and interaction of GRK2 with G-protein-coupled receptors. We established new FRET-based assays to study the interaction of GRK2 with the M_3-ACh receptor (M_3-AChR) as well as G_q-protein subunits with high spatio-temporal resolution in single living HEK293T cells. Combining advantages of FRET imaging with the GRK2 mutants provided new insight into the influence of $G\alpha_q$ on extent and stability of GRK2 interaction with the M_3-AChR.

Molecular Pharmacology Fast Forward. Published on October 14, 2014 as DOI: 10.1124/mol.114.094722
This article has not been copyedited and formatted. The final version may differ from this version.

Materials and Methods

Chemicals

Agar, ampicillin, ECL-solution, and LB-both were purchased from AppliChem (Darmstadt, Germany), acrylamide, glycine, $MgCl_2$, milk powder, SDS, and TEMED from Carl Roth (Karlsruhe, Germany), agarose from Biozym (Hessisch Oldendorf, Germany), $CaCl_2$ from MERCK (Darmstadt, Germany), DMEM, FCS, PBS, penicillin/streptomycin, L-glutamine, and trypsin-EDTA from Biochrom (Berlin, Germany). All other substances were purchased from Sigma-Aldrich (Steinheim, Germany).

Plasmids

The M_3-AChR was obtained from www.cdna.org (#MAR030TN00). cDNAs for $G\alpha_q$, $G\alpha_q$-YFP (Hughes et al., 2001), $G\beta_1$, $G\gamma_2$, α_{2A}-AR, $G\alpha_{i1}$-YFP (C351I) (Bünemann et al., 2003), $G\alpha_{i1}$ (C351I) (Wise et al., 1997), $G\alpha_o$, $G\beta_1$-Cer (Frank et al., 2005), M_3-AChR-YFP (Hoffmann et al., 2012), arrestin3-YFP (Krasel et al., 2005), and GRK2 (Winstel et al., 1996) were described previously. M_3-AChR-mTurq was cloned analogously to M_3-AChR-YFP. M_2-AChR-CFP was generated by cloning CFP with a Ser-Arg linker to the C-terminus of human M_2-AChR. GRK2-YFP and GRK2-mTurq were cloned by fusing the open reading frames of YFP and mTurquoise, respectively, to the C-terminus of human GRK2 using PCR. In these constructs the last amino acid of GRK2 is connected to the second amino acid of the fluorescent protein by a Ser-Arg linker. The GRK2 mutants were generated from these plasmids by site-directed mutagenesis using the following primers: 5' CAAGATGTACGCCATGAGGTGCCTGGACAAAAAG 3' (K220R), 5' CCGGGAGATCTTCGCCTCATACATCATG 3' (D110A), 5' CCTGTTCCCCAACCAGCTGGAGTGGCGGGGCG 3' (R587Q).

Molecular Pharmacology Fast Forward. Published on October 14, 2014 as DOI: 10.1124/mol.114.094722
This article has not been copyedited and formatted. The final version may differ from this version.

Cell culture and transfection

Experiments were performed in HEK293T cells cultured at 37 °C in a humidified atmosphere with 5% CO_2 in Dulbecco´s modified Eagle´s medium (4.5 g/L glucose) supplemented with 10% fetal bovine serum, 2 mM L-glutamine, 100 units/mL penicillin and 0.1 mg/mL streptomycin. Transient transfection was conducted with Qiagen Effectene Transfection Reagent according to the manufacturer's protocol. The general transfection protocol contained 0.5 µg M_3-AChR, 1.6 µg $G\alpha_q$, 0.5 µg $G\beta_1$, 0.2 µg $G\gamma_2$ and 0.5 µg GRK2. In the experiments shown in figure 1, 4 and 6 the protocol was adapted to 1 µg M_3-AChR and 0.1 µg GRK2 to adjust the expression levels. Experiments were performed 40-48h after transfection at room temperature.

Translocation experiments

Translocation experiments were performed with an inverted microscope (IX 71, Olympus) with a 100x oil immersion objective (UPlanSApo 100x/ 1.40 Oil, Olympus) equipped with a confocal FRAP imaging system (VT-HAWK, VisiTech international) and the following filters: T495lpxr, ET 470/40x and ET 535/30m (Chroma). The samples were illuminated with 405 nm and 491 nm lasers (VisiTech international). An Optosplit II with FF560-FDi01, FF01-525/39 and FF01-593/46 (Semrock) was used to split YFP and CFP emission on a CCD camera (EM-CCD Digital Camera, Hamamatsu). Fluorescence recordings were processed using the software VoxCell Scan (VisiTech international). A pressurised perfusion system (Ala-VC^3-8SP, ALA Scientific Instruments) was used to continuously superfuse the cells with buffer (137 mM NaCl, 5.4 mM KCl, 2 mM $CaCl_2$, 1 mM $MgCl_2$, 10 mM Hepes, pH 7.3) or agonist-containing buffer. For translocation experiments GRK2-mTurq-transfected cells were excited at 405 nm and mTurq-emission was recorded at 2 Hz. Subsequently YFP was directly excited at 491 nm and YFP fluorescence recorded at 2 Hz to determine the relative expression level of M_3-AChR and GRK2. To analyse membrane translocation of GRK2 two ROIs were

Molecular Pharmacology Fast Forward. Published on October 14, 2014 as DOI: 10.1124/mol.114.094722
This article has not been copyedited and formatted. The final version may differ from this version.

defined, a polygonal ROI including the cell membrane and a rectangular ROI in the cytosol. Then the quotient $F_{(membrane)}/F_{(cytosol)}$ was calculated. $\Delta(F_{(membrane)}/F_{(cytosol)})$ of the individual recordings was averaged to compare translocation of the different GRK2 mutants.

Single-cell FRET imaging

FRET experiments were performed on an inverted fluorescence microscope (eclipse Ti, Nikon) as described in (Milde et al., 2013). In some experiments cells were not excited with the Lambda DG-4 but with an LED excitation system (pE-2, CoolLED) containing LEDs emitting light at 425 nm and 500 nm, respectively. The intensity of both LEDs was set to 2%. All filters were unchanged. The recording interval is indicated in the figure legend of the respective experiment. Fluorescence data were corrected for background fluorescence, bleed-through and false excitation and the FRET ratio was determined as F_{YFP}/F_{CFP}. The data shown in figure 6A and supplemental Fig. 3 and 4A were additionally corrected for bleaching effects. Individual FRET recordings were averaged and displayed either as absolute alterations in FRET ratio or as data normalised to the individual maximal agonist-induced response in order to compare onset- and offset-kinetics of the agonist induced effect. Absolute alterations in FRET were determined as difference between the averaged FRET ratio of the last ten time points before stimulation with and withdrawal of the agonist for each individual recording. Monoexponential onset- and offset-kinetics were fitted with an exponential function for each individual recording. The obtained k values were used for further statistics. Biexponential kinetics was analysed with the mean traces of the different conditions.

Quantification of relative expression levels

Because of an influence on the extent of the FRET signal the relative expression level of CFP and YFP was controlled. For calibration of the stoichiometry of the relative expression level the construct YFP- β_2-AR-CFP (Dorsch et al., 2009) and analogously cloned reference

Molecular Pharmacology Fast Forward. Published on October 14, 2014 as DOI: 10.1124/mol.114.094722
This article has not been copyedited and formatted. The final version may differ from this version.

constructs with different fluorophores were used. Both fluorophores were excited individually, fluorescence intensities were recorded and corrected for background fluorescence. The calibration factor was calculated as F_{CFP}/F_{YFP}. For each individual FRET-recording the factor F_{CFP}/F_{YFP} was calculated the same way. This factor was divided by the respective calibration factor to calculate the individual expression ratio.

For a reliable comparison of FRET signals the relative expression ratio should not significantly differ between different conditions. An excess of the FRET acceptor YFP is advantageous, as an influence on the extent of the FRET signal is unlikely in that case.

Evaluation and statistics

Data evaluation was conducted with Excel 2010 (Microsoft) and Origin Pro 9.1 (OriginLabs). Arithmetic mean and standard error were calculated where applicable. Statistics were analysed by ANOVA with Bonferroni post-hoc test. p-values < 0.05 were considered to represent significant difference between tested conditions.

Molecular Pharmacology Fast Forward. Published on October 14, 2014 as DOI: 10.1124/mol.114.094722
This article has not been copyedited and formatted. The final version may differ from this version.

Results

Interaction of GRK2 with M_3-AChR

In order to study dynamics of GRK2 interaction with M_3-AChR we set out to image FRET between mTurquoise (mTurq)-labelled M_3-AChR and YFP-labelled GRK2. Functionality of a similarly C-terminally labelled M_3-AChR was described before (Ziegler et al., 2011). The C-terminally YFP-labelled GRK2 was functional, as it phosphorylated rhodopsin similarly to wild-type GRK2 (Supplemental Fig. 1). The fluorescently labelled constructs were transiently transfected in HEK293T cells and subjected to single-cell dual emission FRET recording. mTurq was excited at 425 nm and fluorescence of mTurq and YFP was recorded simultaneously, while cells were continuously superfused with buffer with or without agonist, allowing for determination of onset- and offset-kinetics as a function of agonist addition or withdrawal. Receptor stimulation with a saturating agonist concentration of acetylcholine (ACh, 10 µM) resulted in a reversible increase in YFP fluorescence (yellow trace) and a corresponding decrease in mTurq fluorescence (blue trace), reflecting the development of FRET due to the interaction between GRK2 and the M_3-AChR (Fig. 1A). The emission ratio of both recordings was determined as $\Delta(F_{YFP}/F_{CFP})$ and is in the following referred to as FRET.

The kinase-deficient GRK2(K220R) (Kong et al., 1994), which was used to control for effects due to receptor phosphorylation by GRK2, was comparable to wild-type GRK2 in FRET change (Fig. 1B) and agonist-mediated membrane translocation (Fig. 1C). Therefore, a major influence of receptor phosphorylation on kinetics of GRK2-M_3-AChR interactions can be excluded. To verify specificity of the agonist-dependent alteration of FRET, HEK293T cells were transfected with the same constructs, but additionally with unlabelled α_{2A}-AR and $G\alpha_{i1}$. GRK2 was recruited to the membrane after stimulation with of α_{2A}-AR with 100 µM norepinephrine (NE) (Fig. 1C). However, this membrane recruitment resulted in only a very

Molecular Pharmacology Fast Forward. Published on October 14, 2014 as DOI: 10.1124/mol.114.094722
This article has not been copyedited and formatted. The final version may differ from this version.

minor development of "bystander" FRET between GRK2 and M_3-AChR (Fig. 1B), thereby confirming high specificity of the GRK2-M_3-AChR interaction.

Interaction of GRK2 with $G\alpha_q$-and $G\beta\gamma$

The $G\alpha_q$-protein-binding-attenuated GRK2 variant GRK2(D110A) and the $G\beta\gamma$-binding-attenuated GRK2(R587Q) were used to investigate the effect of $G\alpha_q$-and $G\beta\gamma$ binding by GRK2 on the GRK2-M_3-AChR interaction. To determine the effectiveness of the inserted point mutations, FRET-based interaction assays between GRK2 and $G\beta\gamma$ or $G\alpha_q$ were established in HEK293T cells. M_3-AChR stimulation with 10 µM ACh resulted in a reversible development of FRET that reflects $G\beta\gamma$-GRK2 and $G\alpha_q$-GRK2 interaction (Fig. 2A and B). Between GRK2 and $G\alpha_i$ only a minor rise in FRET was detectable, verifying specificity of the $G\alpha_q$-GRK2 interaction (Supplemental Fig. 2A). GRK2(R587Q) showed a small FRET signal with $G\beta\gamma$, GRK2(D110A) a small FRET signal with $G\alpha_q$ confirming that these mutants exhibit a substantially reduced affinity in respect to the binding of either $G\beta\gamma$ or $G\alpha_q$ or both (Fig. 2C and D, Supplemental Fig. 2B and C). However, $G\alpha_q$-binding-deficiency appeared not as potent as $G\beta\gamma$-binding-deficiency.

Furthermore, the FRET signal between $G\alpha_q$ and GRK2(R587Q) was significantly diminished compared to wild-type GRK2, which confirms the importance of $G\beta\gamma$ for GRK2 translocation. However, $G\alpha_q$ alone recruited a substantial amount of this mutant to the membrane, which argues in favour of a contribution of $G\alpha_q$ to GRK2 recruitment.

Onset-kinetics of the changes in FRET was evaluated by monoexponential fitting. The FRET signal between GRK2 and $G\alpha_q$ ($t_{½}$ = 3.34 s) developed about three times slower than between GRK2 and $G\beta\gamma$ ($t_{½}$ = 0.95 s) (Fig. 2E). This suggests that membrane recruitment of GRK2 by $G\alpha_q$ is delayed compared to $G\beta\gamma$.

Monoexponential fitting did not reveal significant differences in dissociation-kinetics of $G\beta\gamma$ ($t_{½}$ = 25.1 s) and $G\alpha_q$ ($t_{½}$ = 27.1 s) from GRK2. However, the onset of $G\alpha_q$ dissociation was

Molecular Pharmacology Fast Forward. Published on October 14, 2014 as DOI: 10.1124/mol.114.094722
This article has not been copyedited and formatted. The final version may differ from this version.

clearly delayed (Fig. 2F), which argues in favour of a higher binding affinity of GRK2 to $G\alpha_q$ than to $G\beta\gamma$.

Dissociation of $G\beta\gamma$ was significantly accelerated with GRK2(D110A) ($t_{½}$ = 16.3 s), which suggests that $G\alpha_q$ binding affects interaction stability of GRK2 with $G\beta\gamma$.

Both $G\alpha_q$ and $G\beta\gamma$ recruit GRK2 to the membrane

GRK2 membrane translocation was investigated by live-cell confocal microscopy with high temporal resolution. Representative examples demonstrated a clear agonist-dependent membrane targeting of GRK2, GRK2(D110A) and GRK2(R587Q) (Fig. 3A). In contrast the double mutant was barely targeted to the membrane. Statistical evaluation confirmed these observations (Fig. 3B, Supplemental Fig. 2D), suggesting that $G\alpha_q$ as well as $G\beta\gamma$ can recruit GRK2 to the membrane.

Effects of $G\alpha_q$ binding on GRK2-M_3-AChR interaction

Next we tested the contribution of $G\beta\gamma$, $G\alpha_q$ and both together on the interaction of GRK2 with M_3-AChR by means of FRET. Only a minor rise in FRET between M_3-AChR and GRK2 was observed with the $G\beta\gamma$-binding-attenuated GRK2(R587Q) and GRK2(D110A + R587Q) confirming the importance of $G\beta\gamma$ for GRK2 recruitment (Fig. 4A). However, the FRET development was significantly diminished with the $G\alpha_q$-binding-attenuated GRK2(D110A) as well, which supports our hypothesis that $G\alpha_q$ is significantly involved in membrane targeting of GRK2. In this context, it was very important to exclude that the reduction in the amplitude of the FRET signal was due to unfavourable relative expression levels of the fluorescent proteins. Therefore, relative expression levels of GRK2 and M_3-AChR were determined for each individual recording as described in the methods section (Fig. 4B). The results clearly showed that the observed differences in the amplitude of the FRET signal were not due to alterations in the relative expression levels of the fluorescent proteins.

Molecular Pharmacology Fast Forward. Published on October 14, 2014 as DOI: 10.1124/mol.114.094722
This article has not been copyedited and formatted. The final version may differ from this version.

We also compared onset-kinetics and found no significant difference between wild-type GRK2 ($t_{½}$ = 1.44 s) and GRK2(D110A), but significantly slowed onset-kinetics with GRK2(R587Q) ($t_{½}$ = 2.39 s) (Fig. 4C). As GRK2(R587Q), unlike the others, is recruited to the receptor primarily by $G\alpha_q$, these slowed kinetics correspond with the results of the GRK2-G-protein interaction assay that already hint at a delayed membrane targeting of GRK2 by $G\alpha_q$ compared to $G\beta\gamma$ (Fig. 2E). $G\beta\gamma$ binding by GRK2(D110A) ($t_{½}$ = 1.21 s) occurred shortly before M_3-AChR interaction of this mutant ($t_{½}$ = 1.76 s). $G\alpha_q$ binding by GRK2(R587Q) ($t_{½}$ = 2.79 s) was not significantly different from its M_3-AChR interaction ($t_{½}$ = 2.39 s). These data suggest that GRK2 membrane translocation is the rate-limiting step for its receptor interaction.

Dissociation after withdrawal of the agonist proceeded with biphasic kinetics. An initial fast decline was followed by a slower phase that formed the major part (Fig. 4D). This indicates that the majority of GRK2-receptor complexes exhibited a prolonged interaction. GRK2(R587Q) showed a delayed dissociation, which was comparable to the delayed dissociation of $G\alpha_q$ from GRK2. This suggests that in the absence of $G\beta\gamma$-binding the dissociation of GRK2 from the receptor is mostly dependent on the dissociation from $G\alpha_q$. The role of $G\alpha_q$ in GRK2-M_3-AChR interaction was further investigated in the same FRET assay without cotransfection of $G\alpha_q$, $G\beta\gamma$ or the whole heterotrimer. The reduced FRET signal without overexpressed G_q-proteins suggests that the endogenous G-proteins are not sufficient to effectively recruit the exogenous GRK2 to the exogenous receptors (Fig. 4E, Supplemental Fig. 2E). Also with overexpressed $G\alpha_q$ or $G\beta\gamma$ the development of FRET was diminished, which could argue that less functional G_q-proteins were formed. Dissociation of GRK2 was significantly accelerated without overexpressed $G\alpha_q$ suggesting that $G\alpha_q$ binding to GRK2 prolongs interaction of GRK2 with M_3-AChR (Fig. 4F).

Concentration-response-curves

Molecular Pharmacology Fast Forward. Published on October 14, 2014 as DOI: 10.1124/mol.114.094722
This article has not been copyedited and formatted. The final version may differ from this version.

In order to determine the sensitivity of the GRK2 interactions we measured concentration-response curves for $G\alpha_q$-GRK2-, $G\beta\gamma$-GRK2- and M_3-AChR-GRK2 interaction under very similar conditions by utilising the corresponding FRET assays (Fig. 5). Interestingly, the highest sensitivity was observed for the interaction between $G\alpha_q$ and GRK2, which exhibited a concentration-response curve that was significantly left-shifted compared to the $G\beta\gamma$-GRK2 interaction. This argues in favour of a higher binding affinity between GRK2 and $G\alpha_q$ compared to GRK2 and $G\beta\gamma$, which was already suggested by the GRK2-G_q-protein interaction assay (Fig. 2F). The concentration-response-curve of the M_3-AChR-GRK2 interaction was further right-shifted, which can be attributed to the requirement of an active conformation of the receptor. This is known as the spare receptor phenomenon and corresponds well with the concentration-response curve of M_3-AChR activation (Ziegler et al., 2011).

Functional effects of $G\alpha_q$ binding by GRK2

To investigate, whether the effects of $G\alpha_q$ and $G\beta\gamma$ on the GRK2 recruitment influence GRK2 function, we analysed the interaction of arrestin3 with the M_3-ACh receptor by measuring FRET between arrestin3-YFP and M_3-ACh R-mTurq. Arrestin binding to G-protein-coupled receptors requires both GRK-induced receptor phosphorylation (Lohse et al., 1990) and agonist binding to the receptor (Krasel et al., 2005). The latter study describes furthermore that upon agonist washout the GRK2-induced receptor phosphorylation is more sustained than the arrestin binding to the receptor. For this reason arrestin binds very rapidly to prephosphorylated receptors upon repeated stimulation. We confirmed this result with the M_3-AChR and observed an accelerated arrestin recruitment during the second stimulation compared to the first stimulation (Supplemental Fig. 3). Accordingly, arrestin binding to the receptor reflects the GRK2-induced receptor phosphorylation, which demonstrates that real time measurement of arrestin recruitment in response to agonist is a sensitive assay to study

Molecular Pharmacology Fast Forward. Published on October 14, 2014 as DOI: 10.1124/mol.114.094722
This article has not been copyedited and formatted. The final version may differ from this version.

functionality of the different GRK2 mutants. Indeed, in the absence of overexpressed GRK2 or in the presence of the kinase-dead GRK2(K220R) the interaction of arrestin3 with the receptor was significantly reduced compared to wild-type GRK2 (Fig. 6 A, Supplemental Fig. 4A). In these experiments, arrestin3 was always in excess of receptor (Supplemental Fig. 4B), and equal expression of the GRK2 mutants was verified by western blotting (Supplemental Fig. 4C). In the presence of the Gβγ-binding-attenuated and the GRK2 double mutant, arrestin binding was reduced to levels observed in the absence of overexpressed GRK2. This demonstrates that, although the Gβγ-binding-attenuated mutant is able to translocate to the membrane, binding of Gβγ by GRK2 is required for receptor phosphorylation. Importantly, the interaction between receptor and arrestin was significantly diminished in presence of $G\alpha_q$-binding-attenuated GRK2 mutant as well, suggesting that binding of Gβγ and $G\alpha_q$ to GRK2 is required for full kinase function. Onset-kinetics of the arrestin binding to the M_3-AChR appeared faster in presence of wild-type GRK2 compared to the GRK2 mutants, although a detailed analysis was precluded by the increased noise due to the much reduced amplitude in the context of the mutants. In all conditions we observed a fast initial rise in the FRET signal, which presumably can be attributed to arrestin binding to prephosphorylated receptors. However, in cases, where no functional GRK2 was expressed the signal decreased subsequently to various degrees, probably due to competition with either G-proteins or even GRKs. Offset-kinetics after withdrawal of the agonist was not significantly different between the conditions ($t_{½}$ = 2.82 s for GRK2), and markedly faster than dissociation of GRK2 from the receptor.

Having demonstrated that $G\alpha_q$ binding to GRK2 contributes to functional GRK2- M_3-ACh receptor interactions, we wondered whether it also affects interactions of GRK2 with G_i-protein-coupled receptors. We therefore studied the interaction of GRK2 with the G_i-protein-coupled M_2-ACh receptor in presence of the M_3-ACh receptor and overexpressed G_q-proteins. We found no significant difference between the receptor interaction of wild-type GRK2 and

Molecular Pharmacology Fast Forward. Published on October 14, 2014 as DOI: 10.1124/mol.114.094722
This article has not been copyedited and formatted. The final version may differ from this version.

the $G\alpha_q$-binding-attenuated GRK2 mutant, which suggests that $G\alpha_q$ does not contribute to an increased GRK2 binding to G_i-protein-coupled receptors (Fig. 6B, Supplemental Fig. 4D).

Molecular Pharmacology Fast Forward. Published on October 14, 2014 as DOI: 10.1124/mol.114.094722
This article has not been copyedited and formatted. The final version may differ from this version.

Discussion

In the present study we investigated the contributions of $G\alpha_q$ and $G\beta\gamma$ to the agonist-dependent interaction of GRK2 with G_q-protein-coupled receptors and its function. For the first time we were able to observe interactions between GRK2 and receptors or G-protein subunits in real time. $G\alpha_q$ contributed to GRK2 targeting to the membrane, enhanced the extent and stability of the interaction between GRK2 and the M_3-AChR and was important for maximal GRK2 function. These results were obtained from newly established FRET assays using GRK2 and GRK2 point mutants with impaired $G\alpha_q$ or $G\beta\gamma$ interaction. Single cell FRET imaging allowed resolving association and dissociation kinetics in response to fast application or withdrawal of agonist. The loss of function of the $G\alpha_q$- or $G\beta\gamma$-binding-deficient GRK2 mutants employed in this study was verified by FRET experiments (Fig. 2C and D). Each of these mutants contains a point mutation which we consider unlikely to have a major effect on GRK2 interaction with the receptor, the respective unaffected G-protein subunit or overall GRK2 folding. In addition, we controlled expression levels for each recording to ensure comparability of the FRET signals. Confocal imaging demonstrated that interaction of GRK2 with either $G\alpha_q$ or $G\beta\gamma$ was sufficient for membrane targeting upon receptor stimulation (Fig. 3). The role of $G\beta\gamma$ is more prominent which was reflected in faster interaction of GRK2 with $G\beta\gamma$ than with $G\alpha_q$ (Fig. 2E), and in a higher extent of FRET between GRK2 and the receptor for the $G\alpha_q$-binding-attenuated GRK2 mutant than the $G\beta\gamma$-binding-attenuated mutant (Fig. 4A). However, $G\alpha_q$ binding to GRK2 significantly enhanced the extent and stability of the GRK2-M_3-AChR interaction. This was shown by the reduced receptor interaction of the $G\alpha_q$-binding-attenuated GRK2 compared to wild-type GRK2 (Fig. 4A) and by the accelerated dissociation of GRK2 from M_3-AChR after withdrawal of the agonist in the absence of $G\alpha_q$ (Fig. 4F). However, the $G\alpha_q$-binding-attenuated GRK2(D110A) did not dissociate faster from M_3-AChR than wild-type GRK2 (Fig. 4D) which may be explained by the fact that this mutation does only reduce the interaction between GRK2 and

Molecular Pharmacology Fast Forward. Published on October 14, 2014 as DOI: 10.1124/mol.114.094722
This article has not been copyedited and formatted. The final version may differ from this version.

$G\alpha_q$ by about 70%. Furthermore, the affinity between GRK2 and $G\alpha_q$ seemed higher than between GRK2 and $G\beta\gamma$. This was suggested by delayed dissociation of $G\alpha_q$ from GRK2 compared to $G\beta\gamma$ (Fig. 2F) and a significantly higher sensitivity of the GRK2-$G\alpha_q$-interaction than of the GRK2-$G\beta\gamma$-interaction to increasing agonist concentrations (Fig. 5). This may suggest that the contribution of $G\alpha_q$ to GRK2 recruitment is higher at lower agonist concentrations. It has been previously shown that negatively charged phospholipids also play a role in the membrane targeting of GRK2 (Touhara, 1997). Most likely these charged phospholipids will work in concert together with G-protein subunits to recruit GRK2 to membranes and receptors. However, we did not address this issue in the present study. The phospholipid binding sites on GRK2 have been mapped and do not overlap with either the $G\alpha_q$ or the $G\beta\gamma$ binding site (Carman et al., 2000).

It has been shown previously that both agonist occupancy and receptor phosphorylation are necessary for arrestin binding to G-protein-coupled receptors (Krasel et al., 2005). Therefore we used arrestin binding to the M_3-AChR as readout for receptor phosphorylation. $G\beta\gamma$ binding was absolutely required for GRK2 function (Fig. 6A), probably by placing GRK2 and the receptor in a favourable orientation as suggested by previous studies (Wu et al., 1998). In the absence of $G\alpha_q$ binding, some GRK2 activity was retained. However, efficient arrestin recruitment to the M_3-AChR was observed only in the context of interactions of GRK2 with both $G\alpha_q$ and $G\beta\gamma$. We therefore propose that simultaneous binding of GRK2 to $G\beta\gamma$ and $G\alpha_q$ (Tesmer et al., 2005) brings GRK2 in a position where it can optimally phosphorylate the sites on the M_3-AChR that are required for arrestin binding. Accordingly, we hypothesise that dependent on binding of $G\alpha_q$ or $G\beta\gamma$ or both, differential orientations or conformations of GRK2 in the receptor complex exist. In agreement with this hypothesis we observed a delayed dissociation of the $G\beta\gamma$-binding-attenuated GRK2 mutant from the receptor upon

Molecular Pharmacology Fast Forward. Published on October 14, 2014 as DOI: 10.1124/mol.114.094722
This article has not been copyedited and formatted. The final version may differ from this version.

agonist washout (Fig. 4D), which most likely was now dependent on the dissociation of $G\alpha_q$ from GRK2 which was similarly delayed (Fig. 2F).

Comparing the dynamics of GRK2 and arrestin3 interactions with M_3-AChRs we found that surprisingly the dissociation of arrestin from the receptor was much faster than the dissociation of GRK2 (Fig. 4A and 6A). It is generally assumed that receptor phosphorylation does not affect receptor-G-protein coupling and that receptor desensitisation occurs only after binding of arrestins to the receptor (Lohse et al., 1992). However, the prolonged interaction of GRK2 with the M_3-AChR that we observed suggests that, at least for this receptor, G-protein-mediated signalling could already be inhibited by GRK2 binding. Hence, GRK2 presumably contributes to the phosphorylation-independent desensitisation of receptor signalling that was previously attributed to the sequestration of $G\alpha_q$ and $G\beta\gamma$ by GRK2 (Luo et al., 2008).

Taken together, we could visualise interactions of GRK2 with G_q-protein subunits and receptors in single cells and resolve detailed kinetics. Our results uncovered that $G\alpha_q$ binding to GRK2 enhances the recruitment of GRK2 to M_3-ACh receptors. $G\alpha_q$ significantly prolongs the interaction of GRK2 with M_3-AChR, leading to longer occupancy times of receptors, and improves GRK2 function which likely contributes to altered signalling and desensitisation of receptors.

Molecular Pharmacology Fast Forward. Published on October 14, 2014 as DOI: 10.1124/mol.114.094722
This article has not been copyedited and formatted. The final version may differ from this version.

Acknowledgments

Authorship Contributions

Participated in research design: Wolters, Krasel, Brockmann, Bünemann

Conducted experiments: Wolters, Brockmann

Performed data analysis: Wolters, Brockmann, Bünemann

Wrote or contributed to the writing of the manuscript: Wolters, Krasel, Bünemann

Molecular Pharmacology Fast Forward. Published on October 14, 2014 as DOI: 10.1124/mol.114.094722
This article has not been copyedited and formatted. The final version may differ from this version.

References

Bünemann M, Frank M and Lohse MJ (2003) G_i protein activation in intact cells involves subunit rearrangement rather than dissociation. *Proc Natl Acad Sci U S A* **100**: 16077–16082.

Carman CV, Barak LS, Chen C, Liu-Chen LY, Onorato JJ, Kennedy SP, Caron MG and Benovic JL (2000) Mutational analysis of Gβγ and phospholipid interaction with G protein-coupled receptor kinase 2. *J Biol Chem* **275**: 10443–10452.

Carman CV, Parent JL, Day PW, Pronin AN, Sternweis PM, Wedegaertner PB, Gilman AG, Benovic JL and Kozasa T (1999) Selective regulation of $G\alpha_{q/11}$ by an RGS domain in the G protein-coupled receptor kinase, GRK2. *J Biol Chem* **274**: 34483–34492.

Dorsch S, Klotz K, Engelhardt S, Lohse MJ and Bünemann M (2009) Analysis of receptor oligomerization by FRAP microscopy. *Nat Methods* **6**: 225–230.

Fernandez N, Gottardo FL, Alonso MN, Monczor F, Shayo C and Davio C (2011) Roles of phosphorylation-dependent and -independent mechanisms in the regulation of histamine H_2 receptor by G protein-coupled receptor kinase 2. *J Biol Chem* **286**: 28697–28706.

Ford CE, Skiba NP, Bae H, Daaka Y, Reuveny E, Shekter LR, Rosal R, Weng G, Yang CS, Iyengar R, Miller RJ, Jan LY, Lefkowitz RJ and Hamm HE (1998) Molecular basis for interactions of G protein βγ subunits with effectors. *Science* **280**: 1271–1274.

Frank M, Thümer L, Lohse M and Bünemann M (2005) G protein activation without subunit dissociation depends on a $G\alpha_i$-specific region. *J Biol Chem* **280**: 24584–24590.

Hata JA and Koch WJ (2003) Phosphorylation of G protein-coupled receptors: GPCR kinases in heart disease. *Mol Interv* **3**: 264–272.

Hoffmann C, Nuber S, Zabel U, Ziegler N, Winkler C, Hein P, Berlot CH, Bünemann M and Lohse MJ (2012) Comparison of the activation kinetics of the M_3 acetylcholine receptor and a constitutively active mutant receptor in living cells. *Mol Pharmacol* **82**: 236–245.

Hughes TE, Zhang H, Logothetis DE and Berlot CH (2001) Visualization of a functional $G\alpha_q$-green fluorescent protein fusion in living cells. Association with the plasma membrane is disrupted by mutational activation and by elimination of palmitoylation sites, but not be activation mediated by receptors or AlF_4^-. *J Biol Chem* **276**: 4227–4235.

Kong G, Penn R and Benovic JL (1994) A β-adrenergic receptor kinase dominant negative mutant attenuates desensitization of the β_2-adrenergic receptor. *J Biol Chem* **269**: 13084–13087.

Krasel C, Bünemann M, Lorenz K and Lohse MJ (2005) β-arrestin binding to the β_2-adrenergic receptor requires both receptor phosphorylation and receptor activation. *J Biol Chem* **280**: 9528–9535.

Krupnick JG and Benovic JL (1998) The role of receptor kinases and arrestins in G protein-coupled receptor regulation. *Annu Rev Pharmacol Toxicol* **38**: 289–319.

Lohse MJ, Andexinger S, Pitcher J, Trukawinski S, Codina J, Faure JP, Caron MG and Lefkowitz RJ (1992) Receptor-specific desensitization with purified proteins. Kinase dependence and receptor specificity of β-arrestin and arrestin in the β_2-adrenergic receptor and rhodopsin systems. *J Biol Chem* **267**: 8558–8564.

Lohse MJ, Benovic JL, Codina J, Caron MG and Lefkowitz RJ (1990) β-Arrestin: a protein that regulates β-adrenergic receptor function. *Science* **248**: 1547–1550.

Luo J, Busillo JM and Benovic JL (2008) M_3 muscarinic acetylcholine receptor-mediated signaling is regulated by distinct mechanisms. *Mol Pharmacol* **74**: 338–347.

Milde M, Rinne A, Wunder F, Engelhardt S and Bünemann M (2013) Dynamics of $G\alpha_{i1}$ interaction with type 5 adenylate cyclase reveal the molecular basis for high sensitivity of G_i -mediated inhibition of cAMP production. *Biochem J* **454**: 515–523.

Pitcher JA, Freedman NJ and Lefkowitz RJ (1998) G protein-coupled receptor kinases. *Annu Rev Biochem* **67**: 653–692.

Pitcher JA, Inglese J, Higgins JB, Arriza JL, Casey PJ, Kim C, Benovic JL, Kwatra MM, Caron MG and Lefkowitz RJ (1992) Role of βγ subunits of G proteins in targeting the β-adrenergic receptor kinase to membrane-bound receptors. *Science* **257**: 1264–1267.

Raveh A, Cooper A, Guy-David L and Reuveny E (2010) Nonenzymatic rapid control of GIRK channel function by a G protein-coupled receptor kinase. *Cell* **143**: 750–760.

Sallese M, Mariggiò S, D'Urbano E, Iacovelli L and De Blasi A (2000) Selective regulation of G_q signaling by G protein-coupled receptor kinase 2: direct interaction of kinase N terminus with activated $G\alpha_q$. *Mol Pharmacol* **57**: 826–831.

Sterne-Marr R, Tesmer JJG, Day PW, Stracquatanio RP, Cilente JAE, O'Connor KE, Pronin AN, Benovic JL and Wedegaertner PB (2003) G protein-coupled receptor kinase 2/ $G\alpha_{q/11}$ interaction. A novel surface on a regulator of G protein signaling homology domain for binding Gα subunits. *J Biol Chem* **278**: 6050–6058.

Tesmer VM, Kawano T, Shankaranarayanan A, Kozasa T and Tesmer JJG (2005) Snapshot of activated G proteins at the membrane: the $G\alpha_q$-GRK2-Gβγ complex. *Science* **310**: 1686–1690.

Touhara K (1997) Binding of multiple ligands to pleckstrin homology domain regulates membrane translocation and enzyme activity of β-adrenergic receptor kinase. *FEBS Lett* **417**: 243–248.

Touhara K, Koch WJ, Hawes BE and Lefkowitz RJ (1995) Mutational analysis of the pleckstrin homology domain of the β-adrenergic receptor kinase. Differential effects on Gβγ and phosphatidylinositol 4,5-bisphosphate binding. *J Biol Chem* **270**: 17000–17005.

Ungerer M, Bohm M, Elce JS, Erdmann E and Lohse MJ (1993) Altered expression of β-adrenergic receptor kinase and β_1-adrenergic receptors in the failing human heart. *Circulation* **87**: 454–463.

Winstel R, Freund S, Krasel C, Hoppe E and Lohse MJ (1996) Protein kinase cross-talk: membrane targeting of the β-adrenergic receptor kinase by protein kinase C. *Proc Natl Acad Sci U S A* **93**: 2105–2109.

Wise A, Watson-Koken MA, Rees S, Lee M and Milligan G (1997) Interactions of the α_{2A}-adrenoceptor with multiple G_i-family G-proteins: studies with pertussis toxin-resistant G-protein mutants. *Biochem J* **321**: 721–728.

Wu G, Benovic JL, Hildebrandt JD and Lanier SM (1998) Receptor docking sites for G-protein βγ subunits. Implications for signal regulation. *J Biol Chem* **273**: 7197–7200.

Zhong H and Neubig R (2001) Regulation of G protein signaling proteins: Novel multifunctional drug targets. *J Pharmacol Exp Ther* **297**: 837–845.

Ziegler N, Bätz J, Zabel U, Lohse MJ and Hoffmann C (2011) FRET-based sensors for the human M_1-, M_3-, and M_5-acetylcholine receptors. *Bioorg Med Chem* **19**: 1048–1054.

Footnotes

This study was funded by the Collaborative Research Centre SFB 593.

Molecular Pharmacology Fast Forward. Published on October 14, 2014 as DOI: 10.1124/mol.114.094722
This article has not been copyedited and formatted. The final version may differ from this version.

Figure Legends

Figure 1 FRET imaging enables investigation of GRK2 recruitment to M_3-AChR. **(A)** HEK293T cells transiently transfected with YFP-labelled GRK2, M_3-AChR-mTurq, and unlabelled $G\alpha_q$, Gβ and Gγ were subjected to single-cell FRET imaging recorded at 2 Hz. mTurq was excited at 425 nm and mTurq and YFP fluorescence were recorded simultaneously. M_3-AChR stimulation with 10 µM ACh as indicated by the black bar resulted in a reversible increase in YFP fluorescence (yellow trace) and a corresponding decrease in CFP fluorescence (blue trace), reflecting the interaction between GRK2 and M_3-AChR (lower part). The FRET ratio was determined as Δ (F_{YFP}/F_{CFP}) (upper part). **(B)** Single-cell FRET recordings were averaged (mean ± S.E.M.; n≥12) and displayed as absolute alterations in FRET. Experiments with α_{2A}-AR (stimulated with 100 µM NE) and $G\alpha_{i1}$ were used to control signal specificity. The absolute FRET amplitude of the underlying individual experiments was determined as described in the methods section and statistical analysis was performed by ANOVA with Bonferroni posthoc test (*: $p<0.05$). **(C)** Images of the different conditions in the absence and presence of agonist (average of five sequential images recorded by live-cell confocal microscopy).

Figure 2 $G\alpha_q$ binding by GRK2 is delayed compared to Gβγ binding. HEK293T cells transiently transfected with Gβ-Cer, GRK2-YFP, unlabelled M_3-AChR, $G\alpha_q$ and Gγ for the Gβγ-GRK2 interaction assay **(A)** and with $G\alpha_q$-YFP, GRK2-mTurq and unlabelled M_3-AChR, Gβ and Gγ for the $G\alpha_q$-GRK2 interaction assay **(B)** were subjected to single-cell FRET imaging recorded at 2 Hz. M_3-AChR stimulation with 10 µM ACh as indicated led to a development of FRET, reflecting the interaction of GRK2 with Gβ and $G\alpha_q$, respectively (representative recordings in (A) and (B)). Individual single-cell FRET recordings were averaged (mean ± S.E.M.; n≥9) and displayed either as absolute alterations in FRET **(C, D)** or as data normalised to the individual maximal agonist-induced response in order to compare

onset-kinetics **(E)** and offset-kinetics **(F)** of the agonist induced effect. Statistics are given for analysis of absolute amplitudes or kinetics by ANOVA with Bonferroni posthoc test (*: $p<0.05$).

Figure 3 $G\beta\gamma$ or $G\alpha_q$ binding is required for GRK2 membrane translocation. HEK293T cells transiently transfected with mTurq-labelled GRK2 mutants, M_3-AChR-YFP and unlabelled G_q-protein subunits were subjected to live-cell confocal microscopy recorded at 2 Hz. **(A)** Images of different GRK2 mutants in absence and presence of agonist (average of five sequential images). **(B)** Individual recordings (mean ± S.E.M.; $n\geq10$) of GRK2 membrane translocation were evaluated and averaged as described in the methods section.

Figure 4 $G\alpha_q$ improves the extent and stability of agonist-dependent interaction of GRK2 with M_3-AChR. Individual single-cell FRET recordings were averaged (mean ± S.E.M.; $n\geq12$) and displayed either as absolute alterations in FRET **(A)** or as data normalised to the individual maximal agonist-induced response in order to compare onset-kinetics **(C)** and offset-kinetics **(D)** of the agonist induced effect. The trace of wild-type GRK2 was already shown in figure 1B. Statistics are given for analysis of absolute amplitudes or kinetics by ANOVA with Bonferroni posthoc test (*: $p<0.05$). **(B)** Relative expression levels of GRK2 mutants and M_3-AChR in the assay shown in A were not significantly different between the conditions. **(F)** HEK293T cells transiently transfected analogously to A, but either without $G\alpha_q$, $G\beta\gamma$ or the whole heterotrimer were subjected to single-cell FRET imaging recorded at 2 Hz. Individual single-cell FRET recordings were averaged (mean ± S.E.M.; $n\geq12$) and displayed either as absolute alterations in FRET **(E)** or as data normalised to the individual maximal agonist-induced response in order to compare offset-kinetics **(F)** of the agonist induced effect.

Figure 5 Concentration-response curves of the different interaction assays. HEK293T cells transiently transfected as indicated in figures 1 and 2 were subjected to single-cell FRET

imaging recorded at 2 Hz. The M_3-AChR was stimulated with increasing ACh concentrations and the agonist-mediated responses were normalised to the saturating ACh concentration (mean ± S.E.M.; n≥9). log (EC_{50}) of the underlying individual experiments was determined and statistical analysis was performed by ANOVA with Bonferroni posthoc test (*: $p<0.05$). Compared to $G\alpha_q$-GRK2 interaction [log (EC_{50}) = -8.60 ± 0.07, EC_{50} = 2.52 nM ACh] the concentration-response curves of $G\beta\gamma$-GRK2 interaction [log (EC_{50}) = -8.24 ± 0.08, EC_{50} = 5.82 nM ACh] and M_3-AChR-GRK2 interaction [log (EC_{50}) = -7.14 ± 0.09, EC_{50} = 71.9 nM ACh] were significantly right-shifted.

Figure 6 Functional effects of G_q-protein binding to GRK2. **(A)** HEK293T cells transiently transfected with M_3-AChR-mTurq, arrestin3-YFP, unlabelled $G\alpha_q$, $G\beta$, $G\gamma$ and the different GRK2 mutants were subjected to single-cell FRET imaging recorded at 5 Hz. Individual single-cell FRET recordings were corrected for bleaching, averaged (mean ± S.E.M.; n≥13) and displayed as absolute agonist-induced alterations in FRET. Statistics are given for analysis of absolute amplitudes by ANOVA with Bonferroni posthoc test (*: $p<0.05$). **(B)** HEK293T cells transiently transfected with M_2-AChR-CFP, GRK2-YFP or GRK2(D110A), unlabelled M_3-AChR, $G\alpha_q$, $G\alpha_o$, $G\beta$, and $G\gamma$ were subjected to single-cell FRET imaging recorded at 2 Hz. Individual single-cell FRET recordings were averaged (mean ± S.E.M.; n≥14) and displayed as absolute alterations in FRET. Statistics are given for analysis of absolute amplitudes or onset-kinetics by ANOVA with Bonferroni posthoc test (*: $p<0.05$).

Molecular Pharmacology Fast Forward. Published on October 14, 2014 as DOI: 10.1124/mol.114.094722
This article has not been copyedited and formatted. The final version may differ from this version.

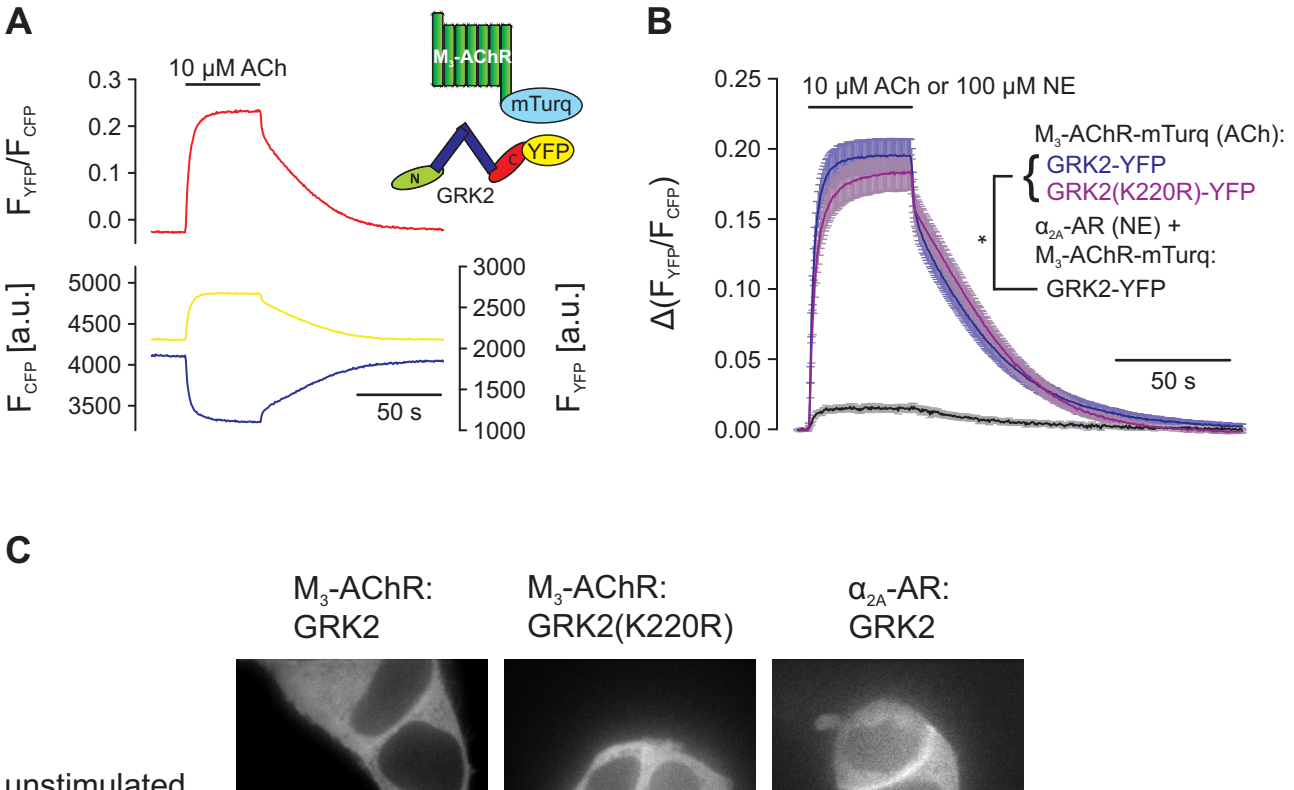

Figure 1

Molecular Pharmacology Fast Forward. Published on October 14, 2014 as DOI: 10.1124/mol.114.094722
This article has not been copyedited and formatted. The final version may differ from this version.

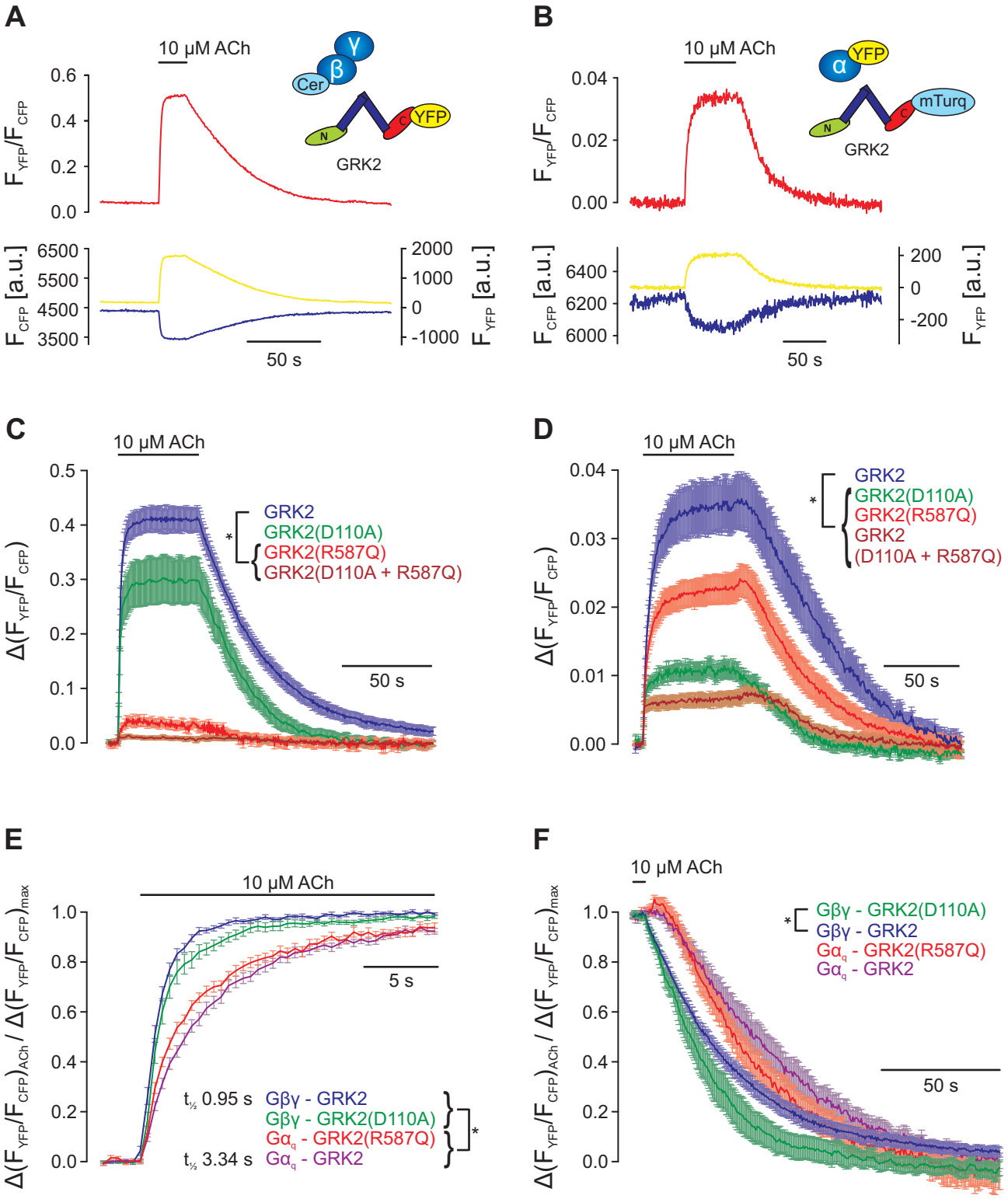

Figure 2

Molecular Pharmacology Fast Forward. Published on October 14, 2014 as DOI: 10.1124/mol.114.094722
This article has not been copyedited and formatted. The final version may differ from this version.

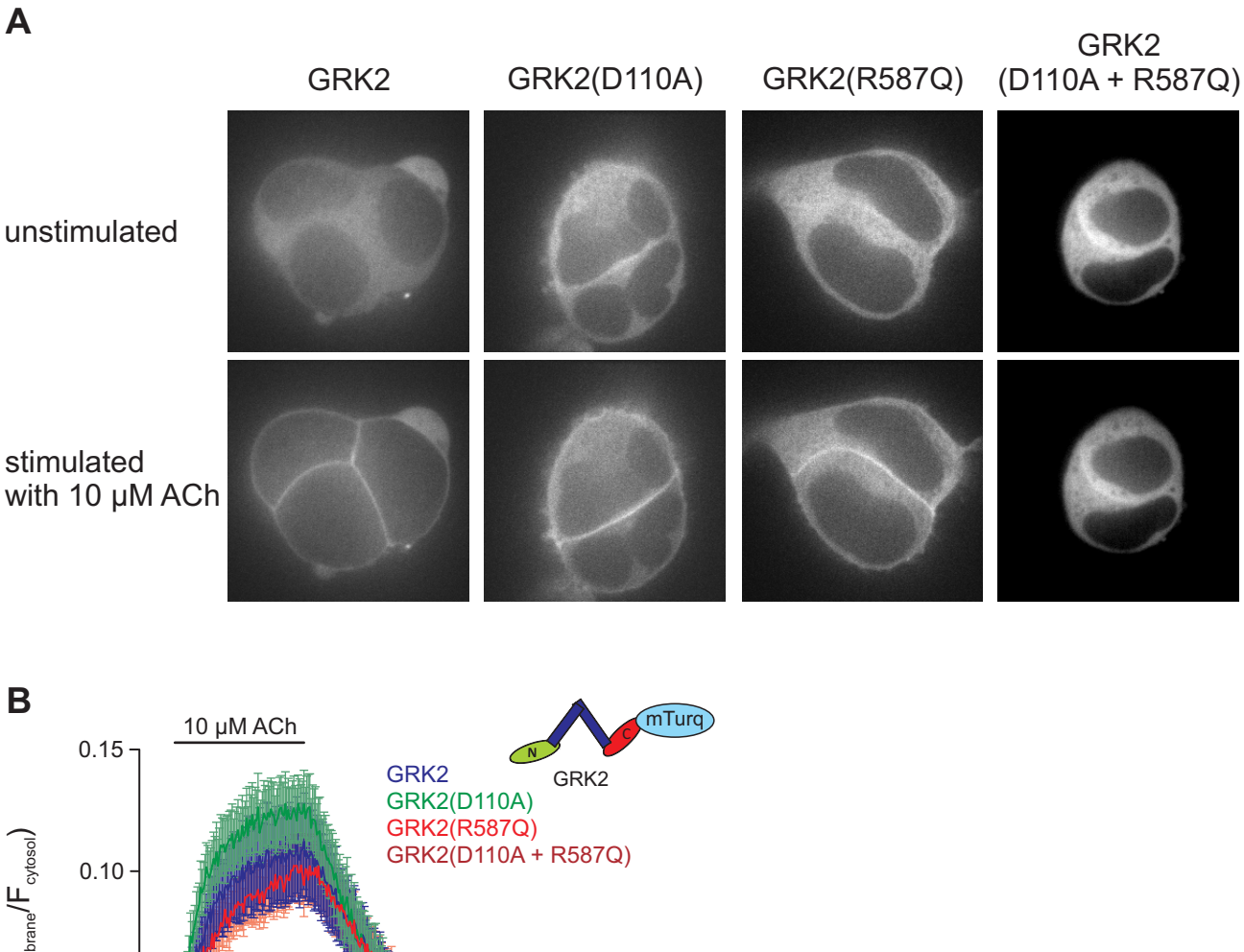

Figure 3

Molecular Pharmacology Fast Forward. Published on October 14, 2014 as DOI: 10.1124/mol.114.094722
This article has not been copyedited and formatted. The final version may differ from this version.

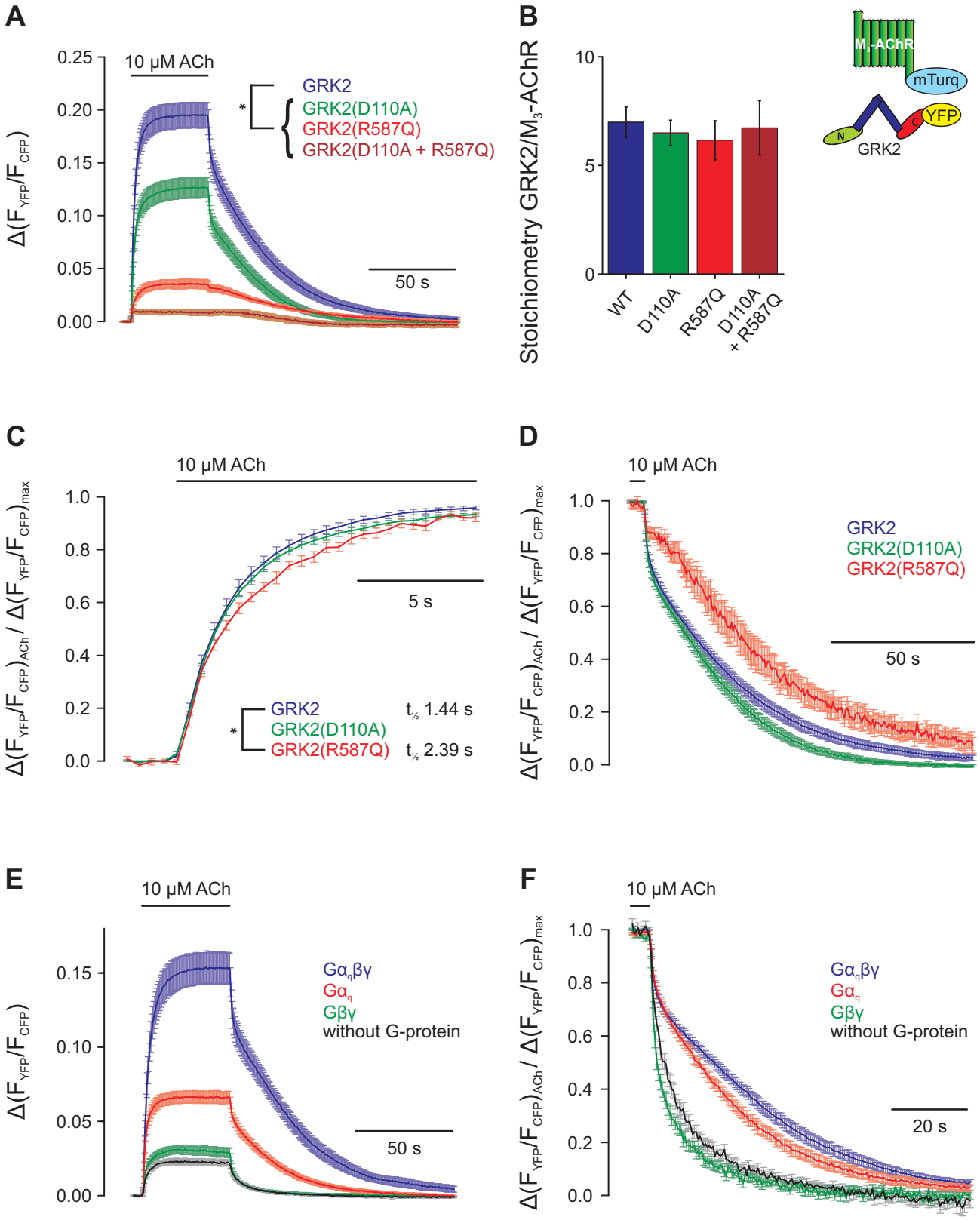

Figure 4

Molecular Pharmacology Fast Forward. Published on October 14, 2014 as DOI: 10.1124/mol.114.094722
This article has not been copyedited and formatted. The final version may differ from this version.

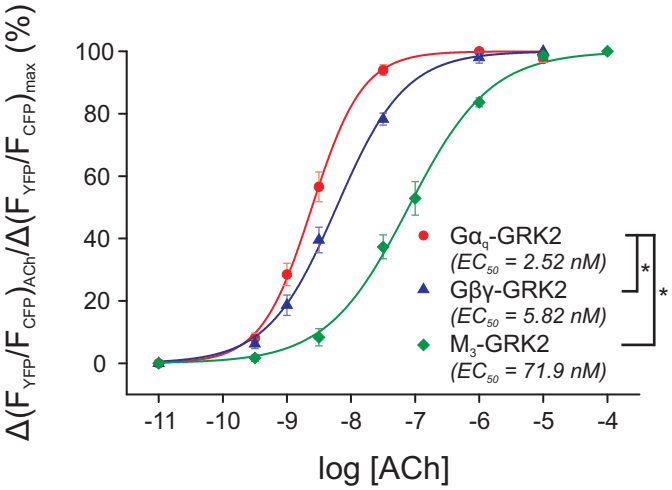

Figure 5

Molecular Pharmacology Fast Forward. Published on October 14, 2014 as DOI: 10.1124/mol.114.094722
This article has not been copyedited and formatted. The final version may differ from this version.

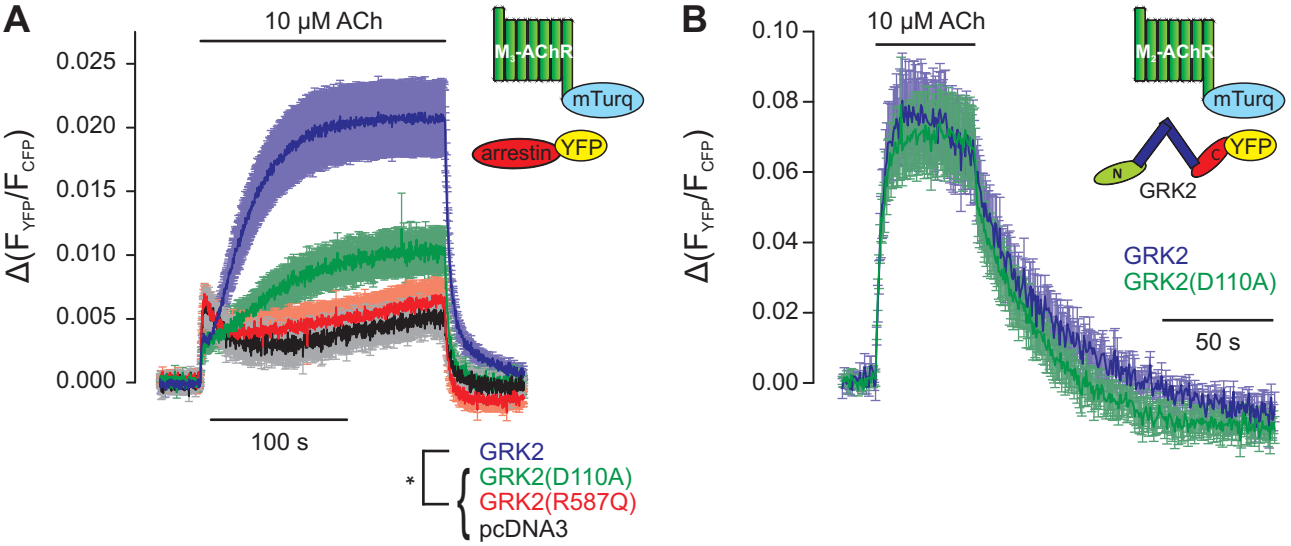

Figure 6